Dexmedetomidine attenuates neuroinflammation and microglia activation in LPS-stimulated BV2 microglia cells through targeting circ-Shank3/miR-140-3p/TLR4 axis

Guangbao He,* Yibo He,* Hongwei Ni, Kai Wang, Yijun Zhu, Yang Bao

Department of Anesthesiology, Jiading District Central Hospital Affiliated Shanghai University of Medicine and Health Sciences, Shanghai, China

*These authors share first authorship

ABSTRACT

It has been shown that dexmedetomidine (Dex) could attenuate postoperative cognitive dysfunction (POCD) *via* targeting circular RNAs (circRNAs). Circ-Shank3 has been found to be involved in the neuroprotective effects of Dex against POCD. However, the role of circ-Shank3 in POCD remains largely unknown. Reverse transcription quantitative PCR (RT-qPCR) was performed to detect circ-Shank3 and miR-140-3p levels in lipopolysaccharide (LPS)-treated microglia BV-2 cells in the absence or presence of Dex. The relationship among circ-Shank3, miR-140-3p and TLR4 was confirmed by dual-luciferase reporter assay. Additionally, Western blot and immunofluorescence assays were conducted to evaluate TLR4, p65 and Iba-1 or CD11b levels in cells. In this study, we found that Dex notably decreased circ-Shank3 and TLR4 levels and elevated miR-140-3p level in LPS-treated BV2 cells. Mechanistically, circ-Shank3 harbor miR-140-3p, functioning as a miRNA sponge, and then miR-140-3p targeted the 3'-UTR of TLR4. Additionally, Dex treatment significantly reduced TLR4 level and phosphorylation of p65, and decreased the expressions of microglia markers Iba-1 and CD11b in LPS-treated BV2 cells. As expected, silenced circ-Shank3 further reduced TLR4, p65 and Iba-1 and CD11b levels in LPS-treated BV2 cells in the presence of Dex, whereas these phenomena were reversed by miR-140-3p inhibitor. Collectively, our results found that Dex could attenuate the neuroinflammation and microglia activation in BV2 cells exposed to LPS *via* targeting circ-Shank3/miR-140-3p/TLR4 axis. Our results might shed a new light on the mechanism of Dex for the treatment of POCD.

Key words: postoperative cognitive dysfunction; neuroinflammation; circRNAs; TLR4.

Correspondence: Yang Bao, Department of Anesthesiology, Jiading District Central Hospital Affiliated Shanghai University of Medicine & Health Sciences, No. 1 Chengbei Road, Jiading District, Shanghai 201800, China.
E-mail: baoyang_BY@126.com

Contributions: GH, YH, made major contributions to the design and manuscript drafting of this study; HN, KW, YZ, were responsible for data acquisition, data analysis and manuscript revision; YB, made substantial contributions to conception of the study and revised the manuscript critically for important intellectual content. All the authors read and approved the final version of the manuscript and agreed to be accountable for all aspects of the work.

Conflict of interest: the authors declare that they have no competing interests, and all authors confirm accuracy.

Funding: 1. Shanghai Municipal Jiading District New Key Subject Program (2020-jdyxzdxk-03). 2. Shanghai Municipal Jiading District Natural Science Research Program (JDKW-2020-0012). 3. Shanghai Municipal Jiading District Natural Science Research Program (JDKW-2021-0036).

Introduction

Postoperative cognitive dysfunction (POCD) is a common complication following anesthesia and surgical intervention, which is characterized by memory loss and cognitive impairment.[1,2] POCD severely impacts patients' quality of life, especially in older patients.[3] Surgery-induced neuroinflammation plays a pivotal role in POCD, which has become a hallmark of POCD.[4,5] Surgery often leads to increased production of systemic proinflammatory factors including IL-lβ, IL-6 and TNF-α, and then incites neuroinflammation, eventually resulting in neuronal dysfunction and cognitive decline.[6,7] Conversely, inhibition of neuroinflammation could improve cognitive dysfunction and attenuate POCD development.[8] Our previous study showed that dexmedetomidine (Dex), a selective α2-adrenergic agonist, could suppress inflammation response in microglial BV2 cells exposed to LPS.[9] Moreover, Dex could exhibit neuroprotective effects against POCD.[10] However, the mechanisms by which Dex attenuates POCD development is not clearly understood.

Circular RNAs (circRNAs) are covalently closed RNA molecules characterized by their covalently closed-loop structures.[11] CircRNAs can regulate gene expressions through functioning as microRNAs (miRNAs) sponges.[12] Additionally, circRNAs can exert important roles in the pathological progressions of many diseases including POCD.[13] Qian *et al.* found that downregulation of circUBE3B could attenuate sevoflurane-induced neuron injury through targeting miR-326.[14] Additionally, Dex could reduce circ-Shank3 level in aged POCD rats;[15] thus, circ-Shank3 may participate in the neuroprotective effects of Dex against POCD. However, the role of circ-Shank3 in POCD remains largely unknown. MiR-140-3p was reported to participate in regulating cellular inflammatory processes.[16,17] Wu *et al*. found that miR-140-3p could attenuate sevoflurane-induced POCD in rats.[18] Additionally, miR-140-3p could regulate cellular inflammatory response *via* targeting TLR4.[19] Moreover, inhibiting TLR4/NF-κB signaling was able to weaken neuroinflammation in glaucoma.[20] However, the relationship among circ-Shank3, miR-140-3p and TLR4/NF-κB signaling remains unclear. Therefore, in this study, we aimed to explore whether Dex could reduce LPS-induced inflammation response in BV2 cells by targeting circ-Shank3/miR-140-3p/TLR4 axis.

Materials and Methods

Cell culture and treatment

The mouse microglial BV2 cells were purchased from the Shanghai Zhong Qiao Xin Zhou Biotechnology Co., Ltd. (Shanghai, China). Cells were cultured in Minimum Essential Medium (Gibco, Billings, MT, USA) containing 10% FBS and 1% penicillin/streptomycin in a humidified atmosphere containing 5% CO_2 at 37°C. Once the BV2 cells reached 80% cell confluence, cells were treated with Dex (20 μg/mL) for 30 min and then treated with LPS (10 μg/mL) for 24 h, as previously described.[9]

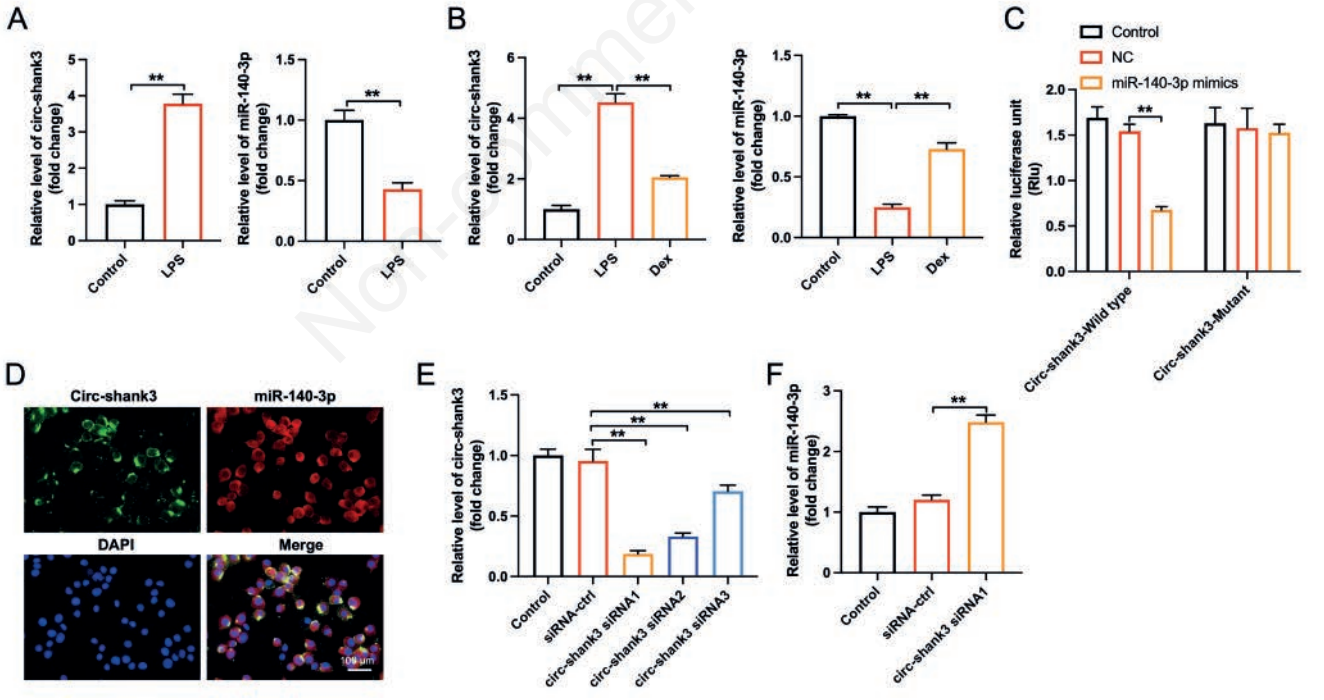

Figure 1. Circ-Shank3 acts as the sponge of miR-140-3p. **A**) RT-qPCR analysis of circ-Shank3 or miR-140-3p level in LPS-treated BV2 cells. **B**) BV2 cells were treated with 20 μg/mL Dex, followed by treatment with 10 μg/mL LPS; RT-qPCR analysis of circ-Shank3 or miR-140-3p level in BV2 cells. **C**) Luciferase reporter assay showed the molecular combination of miR-140-3p with circ-Shank3 wild type. **D**) The location of circ-Shank3 (green color) and miR-140-3p (red color) were detected by FISH analysis; DAPI, blue color. **E**) RT-qPCR analysis of circ-Shank3 level in BV2 cells transfected with siRNA-ctrl, circ-Shank3 siRNA1, siRNA2 or siRNA3. **F**) RT-qPCR analysis of miR-140-3p level in BV2 cells transfected with siRNA-ctrl or circ-Shank3 siRNA1. **p<0.01.

Cell transfection

MiR-140-3p mimics, miR-140-3p inhibitor, miRNA negative control (NC) and circ-Shank3 siRNA (circ-Shank3 siRNA1, circ-shank3 siRNA2 and circ-Shank3 siRNA3) and siRNA NC were purchased from Ribobio. Once the BV2 cells reached 80% cell confluence, cells were transfected with miR-140-3p mimics (5'-UACCACAGGGUAGAACCACGG-3'), miR-140-3p inhibitor (5'-CCGUGGUUCUACCCUGUGGUA-3'), circ-Shank3 siRNA1 (5'- TGTCCCTATTCAGATGGCATCTGTA-3'), circ-shank3 siRNA2 (5'- GCAAAGGAAGCTTTCTGCAGTATAT-3') or circ-shank3 siRNA3 (5'- CAGTCAGAGTTTGGGTCCT-GTTCCA-3') using Lipofectamine 2000.[21]

Reverse transcription quantitative PCR (RT-qPCR)

Total RNA was extracted with the TRIpure Total RNA Extraction Reagent (EP013). Next, RNA was reverse transcribed to cDNAs using the EntiLink™ 1st Strand cDNA Synthesis Kit (EQ003) and qPCR process was carried out using EnTurbo™ SYBR Green PCR SuperMix (EQ001) on the instrument of QuantStudio 6 Flex Real-Time PCR System (Life Technologies, Carlsbad, CA, USA). Data were normalized to U6 or β-actin. The $2^{-\Delta\Delta Ct}$ method was applied to calculate the relative gene level.

U6 forward, 5'-CTCGCTTCGGCAGCACAT-3' and reverse, 5'-AACGCTTCACGAATTTGCGT; miR-140-3p forward, 5'- GCC-TACCACAGGGTAGAACC-3' and reverse, 5'- CTCAACTGGT-GTCGTGGAGTC-3'; GAPDH forward, 5'- CATCATCCCTGCCTC-TACTGG-3' and reverse, 5'- GTGGGTGTCGCTGTTGAAGTC-3'; circ-Shank3 forward, 5'- TGAATAAAGACACACGCTCCTT-3' and reverse 5'-CTGATCTCAGCAGGGGTGATC-3'; TLR4 forward, 5'-ACACTTTATTCAGAGCCGTTGGT-3' and reverse, 5'- CAGGTC-CAAGTTGCCGTTTC-3'.

Dual-luciferase reporter assay

Wild-type and mutant circ-shank3, the 3′-untranslated region (3′-UTR) of TLR4 fragments were constructed and subcloned into the luciferase reporter vector. BV2 cells were co-transfected with the above reporter gene plasmids and miR-140-3p mimics or NC, respectively. Next, a dual-luciferase reporter system kit (Promega, Madison, WI, USA) was applied for detecting the luciferase activity in BV2 cells.

Fluorescence *in situ* hybridization

The FITC-labeled circ-Shank3 FISH probe and Cy3-labeled miR-140-3p FISH probe were obtained from RiboBio (Guangzhou, China). Cells were fixed in 4% paraformaldehyde, blocked with the pre-hybridization buffer for 1 h at 37°C and then incubated with hybridization buffer containing the circ-Shank3 and miR-140-3p probes at 37°C overnight. Next, the saline sodium citrate buffer was used to wash the cells, and images were photographed by confocal microscopy (LSM880, objective: 40x, light: laser; Zeiss, Oberkochen, Germany). Nuclei were stained with DAPI (10 μg/mL) for 30 min in darkness.

Western blot assay

The protein concentration was determined using the BCA pro-

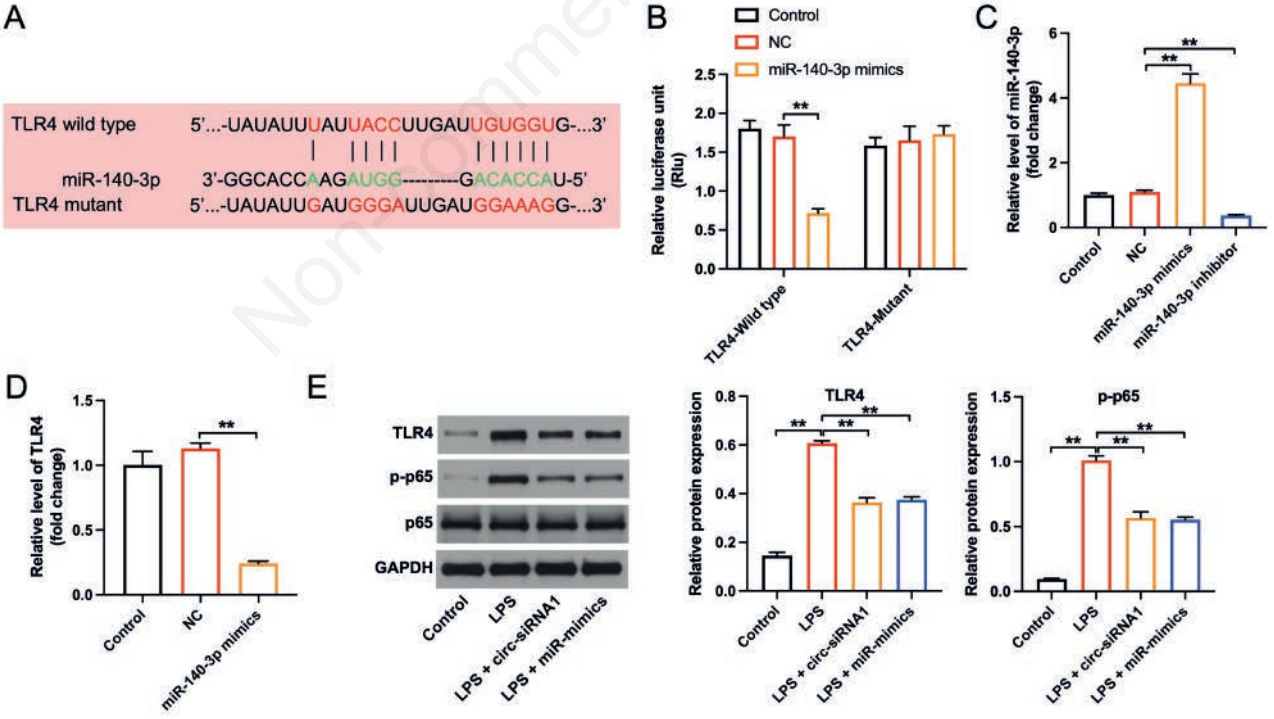

Figure 2. Circ-Shank3/miR-140-3p targets TLR4 in BV2 cells. **A**) The potential binding site of miR-140-3p and TLR4. **B**) Luciferase reporter assay showed the molecular combination of miR-140-3p with TLR4 mRNA wild type. **C**) RT-qPCR analysis of miR-140-3p level in BV2 cells transfected with NC, miR-140-3p mimics or miR-140-3p inhibitor. **D**) RT-qPCR analysis of TLR4 mRNA level in BV2 cells transfected with NC or miR-140-3p mimics. **E**) BV2 cells were transfected with miR-140-3p mimics or circ-Shank3 siRNA1, followed by treatment with 10 μg/mL LPS. Western blot analysis of TLR4, p-p65 and p65 protein expressions in BV2 cells. **p<0.01.

tein concentration detection kit (Aspen, Wuhan, China). Equal amounts of proteins were then separated on 10% SDS-PAGE and electroblotted onto a PVDF membrane. Next, the membrane was incubated overnight at 4°C with the primary antibodies: anti-TLR4 (19811-1-AP, 1:1000; Proteintech, Rosemont, IL, USA), anti-p-NF-κB p65 (#3033, 1:500; Cell Signaling Technology, Danvers, MA, USA), anti-NF-κB p65 (#8242, 1:3000; Cell Signaling Technology), and GAPDH (ab181602, 1:10000; Abcam, Cambridge, UK). After that, the membrane was probed with a secondary antibody (AS1107, 1:10000; Aspen) at room temperature. Subsequently, the bands were developed with an enhanced chemiluminescence detection kit (Aspen) and the band intensity was analyzed using the AlphaEaseFC software.

Immunofluorescence assay

BV2 cells were fixed in 4% paraformaldehyde for 20 min, and then incubated with the primary antibodies, such as anti-CD11b antibody (DF2911, 1:200; Affinity Biosciences, Cincinnati, OH, USA), anti-Iba-1 antibody (GB11105, 1:200; Wuhan Servicebio Technology Co., Ltd., Wuhan, China), anti-TLR4 antibody (19811-1-AP, 1:200); Proteintech, anti-NF-κB p65 antibody (#6956, 1:200; Cell Signaling Technology,) and anti-BNDF antibody (ab205067, 1:100; Abcam) overnight at 4°C. Next, cells were probed with corresponding secondary antibodies (1:100; Aspen) such as Cy3-labeled goat anti-rabbit (AS-1109) or Cy3-labeled goat anti-mouse secondary antibodies (AS1111) for 40 min in

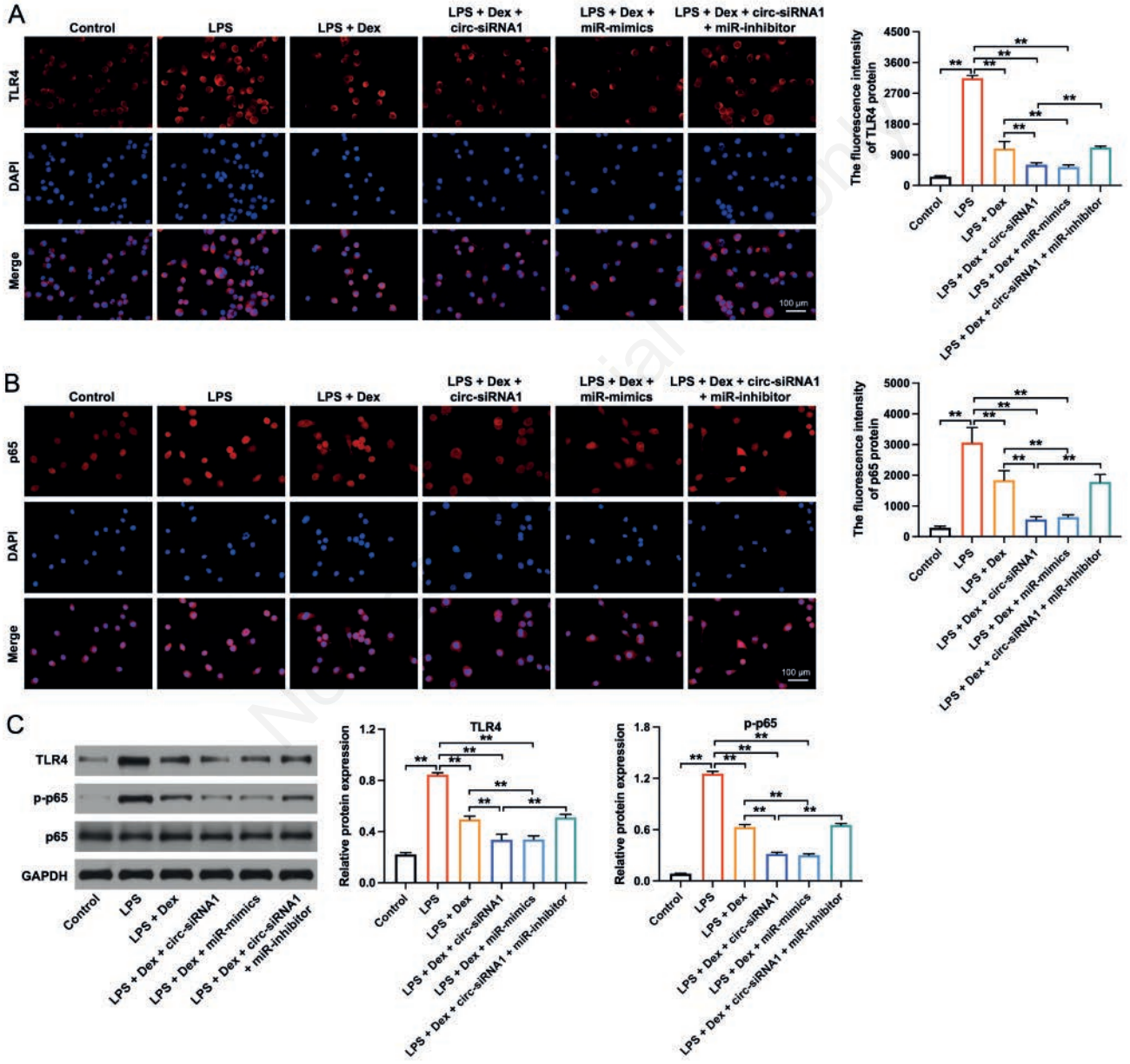

Figure 3. Dex attenuates neuroinflammation in BV2 cells exposed to LPS through modulating circ-Shank3/miR-140-3p/TLR4/NF-κB axis. BV2 cells were treated with 20 μg/mL Dex plus miR-140-3p mimics, circ-Shank3 siRNA1 or circ-Shank3 siRNA1 + miR-140-3p inhibitor, followed by treatment with 10 μg/mL LPS. **A,B**) Immunofluorescence assay was used to estimate the expression of TLR4 and p65 in BV2 cells, based on the fluorescence intensity; TLR4 or p65, red color; DAPI, blue color. **C**) Western blot analysis of TLR4, p-p65 and p65 protein expressions in BV2 cells. **p<0.01.

darkness. Thereafter, DAPI reagent (10 μg/mL) was used for staining the nucleus for 30 min in darkness. Finally, images were then taken by a fluorescence microscope (Eclipse Ci-L, objective: 40x, light: mercury lamp; Nikon, Tokyo, Japan). As negative control, the primary antibody was omitted. The fluorescence intensity of each image was quantified by Image-Pro Plus software.

ELISA

ELISA kits obtained from ELK Biotechnology (Wuhan, China) were used to detect the levels of TNF-α (ELK1395), IL-1β (ELK1271), IL-6 (ELK1157) in cell culture supernatants according to the manufacturer's recommendations. Meanwhile, malondialdehyde (MDA) level in cell culture supernatants was measured by the MDA assay kit (A003-1; Nanjing Jiancheng Bioengineering Institute, Nanjing, China).

Statistical analysis

All of the experiments were repeated at least three times. One-way analysis of variance (ANOVA) followed by Tukey's tests were used for comparisons between groups. All data are shown as the mean±standard deviation. $p<0.05$ was considered statistically significant.

Results

Circ-Shank3 acts as a sponge of miR-140-3p

It has been shown that circ-Shank3 and miR-140-3p play key roles in POCD development.[15,18] To explore whether circ-Shank3 could serve as a sponge for miR-140-3p in BV2 cells, circ-Shank3 and miR-140-3p levels in LPS-treated BV2 cells were detected by RT-qPCR. As shown in Figure 1 A,B, circ-Shank3 level was significantly elevated and miR-140-3p level was notably reduced in LPS-treated BV2 cells; however, Dex treatment obviously declined circ-Shank3 level and elevated miR-140-3p level in LPS-treated BV2 cells. Additionally, the luciferase reporter assay results showed that miR-140-3p mimics markedly reduced the luciferase activity of wild-type circ-Shank3 in BV2 cells (Figure 1C), suggesting that circ-Shank3 closely combined with miR-140-3p. Moreover, the results of FISH assay showed that circ-Shank3 and miR-140-3p were both primarily located in the cytoplasm (Figure 1D). Meanwhile, downregulation of circ-Shank3 remarkably declined circ-Shank3 level, but increased miR-140-3p level in BV2 cells (Figure 1 E,F). These findings showed that circ-Shank3 could act as the sponge of miR-140-3p.

Circ-Shank3/miR-140-3p targets TLR4 in BV2 cells

Next, the data in targetScan database showed that TLR4 might be a potential target of miR-140-3p (Figure 2A). Moreover, miR-140-3p mimics obviously inhibited the luciferase activity of wild-type TLR4 in BV2 cells (Figure 2B). RT-qPCR results showed that miR-140-3p mimics strongly increased miR-140-3p level in BV2 cells, whereas miR-140-3p inhibitor obviously declined miR-140-3p level in cells (Figure 2C). Moreover, miR-140-3p mimics markedly reduced the level of TLR4 in BV2 cells (Figure 2D). These results suggested that TLR4 is a downstream target of miR-140-3p. Furthermore, LPS significantly upregulated TLR4 and p-p65 protein expressions in BV2 cells; however, circ-Shank3 siRNA1 or miR-140-3p mimics obviously reversed these changes (Figure 2E). Collectively, downregulation of circ-Shank3 or overexpression of miR-140-3p could inhibit TLR4/NF-κB signaling in LPS-treated BV2 cells.

Dex attenuates neuroinflammation in BV2 cells exposed to LPS through modulating circ-Shank3/miR-140-3p/TLR4/NF-κB axis

Activating TLR4/NF-κB signaling could induce neuroinflammation in POCD.[22,23] Thus, to further explore whether Dex could inhibit TLR4/NF-κB signaling in BV2 cells *via* targeting circ-Shank3/miR-140-3p axis, IF and Western blot assays were conducted. The results showed that Dex treatment significantly reduced TLR4 protein level and the total and phosphorylated p65 protein expressions in LPS-treated BV2 cells (Figure 3 A-C). As expected, circ-Shank3 downregulation further reduced TLR4 and

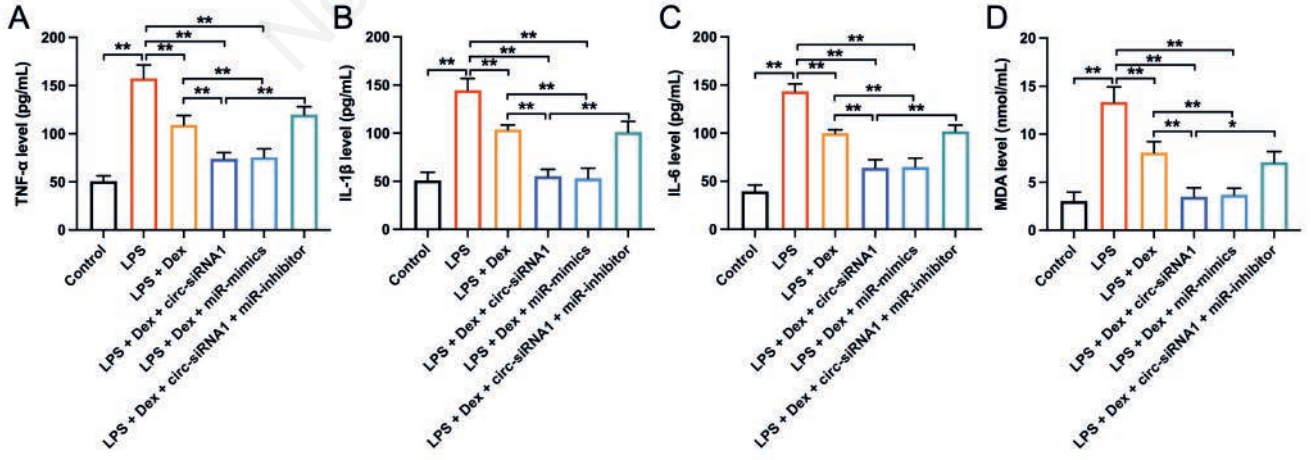

Figure 4. Dex reduces pro-inflammatory cytokines in BV2 cells exposed to LPS through modulating circ-Shank3/miR-140-3p axis. BV2 cells were treated with 20 μg/mL Dex plus miR-140-3p mimics, circ-Shank3 siRNA1 or circ-Shank3 siRNA1 + miR-140-3p inhibitor, followed by treatment with 10 μg/mL LPS. **A-D**) ELISA analysis of TNF-α, IL-1β, IL-6 and MDA levels in the culture supernatant of BV2 cells. *p<0.05, **p<0.01.

p65 levels in LPS-treated BV2 cells in the presence of Dex; however, these phenomena were reversed by miR-140-3p inhibitor (Figure 3 A-C). Additionally, Dex treatment notably reduced TNF-α, IL-1β, IL-6 and MDA levels in LPS-treated BV2 cells. Meanwhile, circ-Shank3 siRNA1 further reduced TNF-α, IL-1β, IL-6 and MDA levels in LPS-treated BV2 cells in the presence of Dex; however, these levels were reversed by miR-140-3p inhibitor (Figure 4 A-D). Collectively, Dex could attenuate neuroinflammation in LPS-treated BV2 cells by modulating circ-Shank3/miR-140-3p/TLR4/NF-κB axis.

Dex attenuates LPS-induced microglia activation through modulating circ-Shank3/miR-140-3p axis

Furthermore, LPS notably increased CD11b and Iba-1 levels and declined BDNF in BV2 cells (Figure 5 A-C). However, Dex treatment obviously declined CD11b and Iba-1 levels, and increased BDNF level in LPS-treated BV2 cells (Figure 5 A-C), suggesting that Dex could attenuate LPS-induced microglia activation. As expected, downregulation of circ-Shank3 further decreased CD11b and Iba-1 levels and increased BDNF level in LPS-treated BV2 cells in the presence of Dex; however, these phenomena were reversed by miR-140-3p inhibitor (Figure 5 A-C). Collectively, Dex could attenuate LPS-induced microglia activation in BV2 cells through modulating circ-Shank3/miR-140-3p axis.

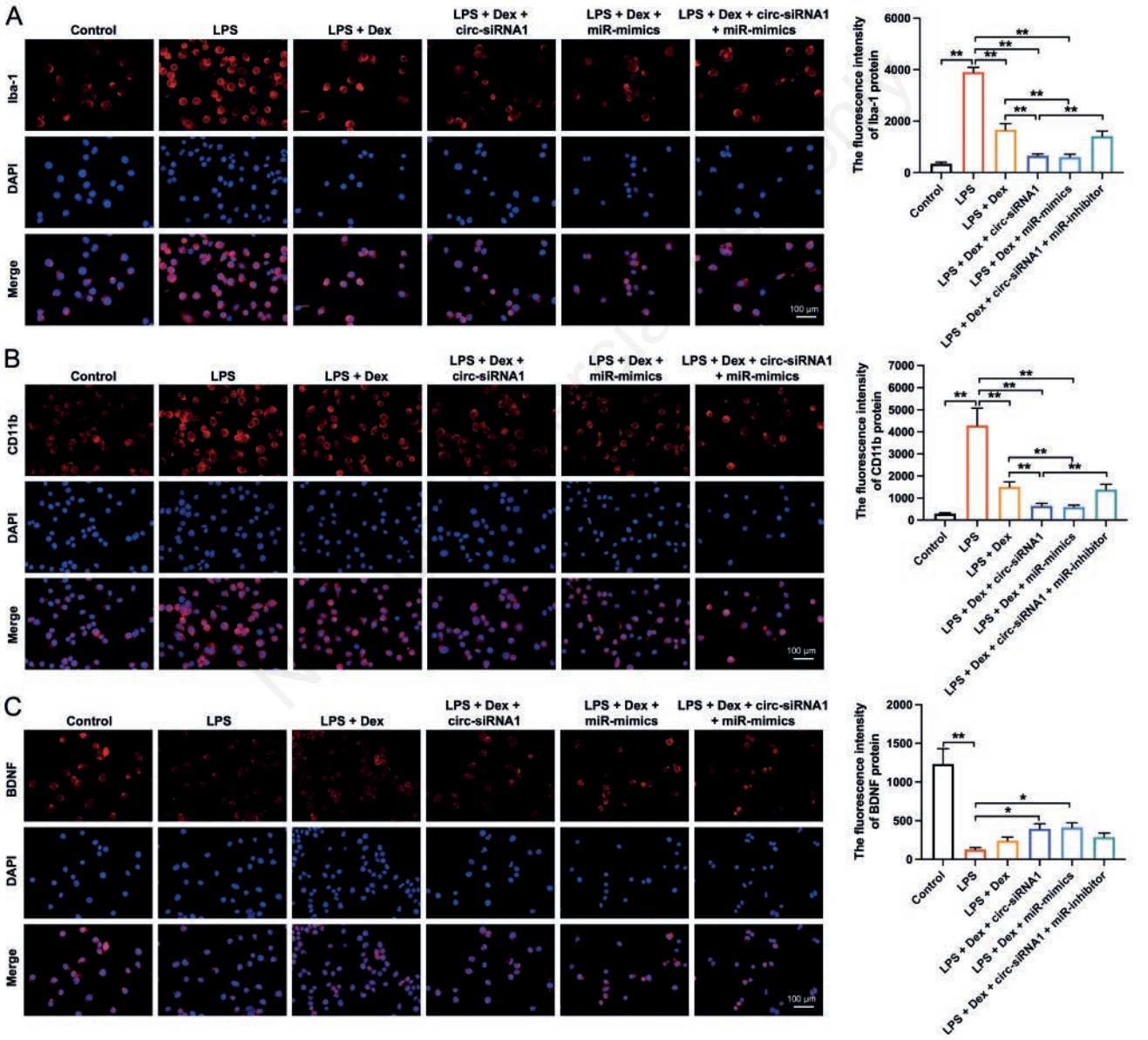

Figure 5. Dex attenuates LPS-induced microglia activation by modulating circ-Shank3/miR-140-3p axis. BV2 cells were treated with 20 μg/mL Dex plus miR-140-3p mimics, circ-Shank3 siRNA1 or circ-Shank3 siRNA1 + miR-140-3p inhibitor, followed by treatment with 10 μg/mL LPS. **A-C**) Immunofluorescence assay was used to estimate the expression of Iba-1, CD11b and BDNF in BV2 cells, based on the fluorescence intensity; Iba-1, CD11b or BDNF, red color; DAPI, blue color. *p<0.05, **p<0.01.

Discussion

Dex, a neuroprotective agent, was shown to exhibit sedative, analgesic, anxiolytic, and neuroprotective effects in some situations.[24,25] Dex could promote spatial learning and memory in rat pups through upregulation of GDNF.[26] Lv *et al*. found that Dex could attenuate cerebral ischemic injury in rats with middle cerebral artery occlusion.[27] Additionally, Dex could improve cognitive dysfunction and neuroinflammation in POCD mice through modulating HDAC2/HIF-1α/PFKFB3 axis.[28] However, the detailed mechanism of Dex in POCD remains largely unknown. Our previous study showed that Dex could ameliorate neuroinflammation in BV2 cells exposed to LPS *via* targeting miR-340.[9] Microglia, the resident cells of the brain, plays key roles in the development and maintenance of brain.[29-31] However, abnormal microglial activation could mediate neuroinflammation and neurodegeneration, leading to several neurological disorders.[32,33] Remarkably, Dex could inhibit microglia activation in mice with spinal cord ischemia-reperfusion injury.[34] In this study, LPS significantly upregulated the expressions of Iba-1 and CD11b in BV2 cells, whereas Dex treatment notably decreased Iba-1 and CD11b levels in LPS-treated BV2 cells. These data suggested that Dex could inhibit microglia activation in LPS-treated BV2 cells, which was consistent with the previous study.

CircRNAs play important roles in the development of POCD.[35] Cao *et al.* reported that Dex could reduce circ-Shank3 level in aged POCD rats, suggesting that circ-Shank3 may be involved in the process of Dex improved POCD.[15] In this study, our results showed that Dex obviously reduced circ-Shank3 level in BV2 cells exposed to BV2 cells. Additionally, circ-Shank3 downregulation or Dex markedly declined Iba-1, CD11b, TNF-α, IL-1β and IL-6 levels in LPS-treated BV2 cells. Meanwhile, downregulation of circ-Shank3 further enhanced Dex-elicited changes in Iba-1, CD11b, TNF-α, IL-1β and IL-6 levels in LPS-treated BV2 cells. Collectively, Dex could protect against LPS-induced microglia activation and neuroinflammation *via* downregulating circ-Shank3. Furthermore, miR-140-3p level was obviously reduced in POCD rats.[18] Overexpression of miR-140-3p could alleviate POCD in rats through inhibiting neuron pyroptosis.[18] Consistent with the previous study, we found that LPS significantly declined miR-140-3p level in BV2 cells; however, Dex treatment elevated miR-140-3p level in LPS-treated BV2 cells. Moreover, overexpression of miR-140-3p further decreased Iba-1, CD11b, TNF-α, IL-1β and IL-6 levels in LPS-treated BV2 cells in the present of Dex. These data suggested that miR-140-3p level was related to the neuroprotective effects of Dex.

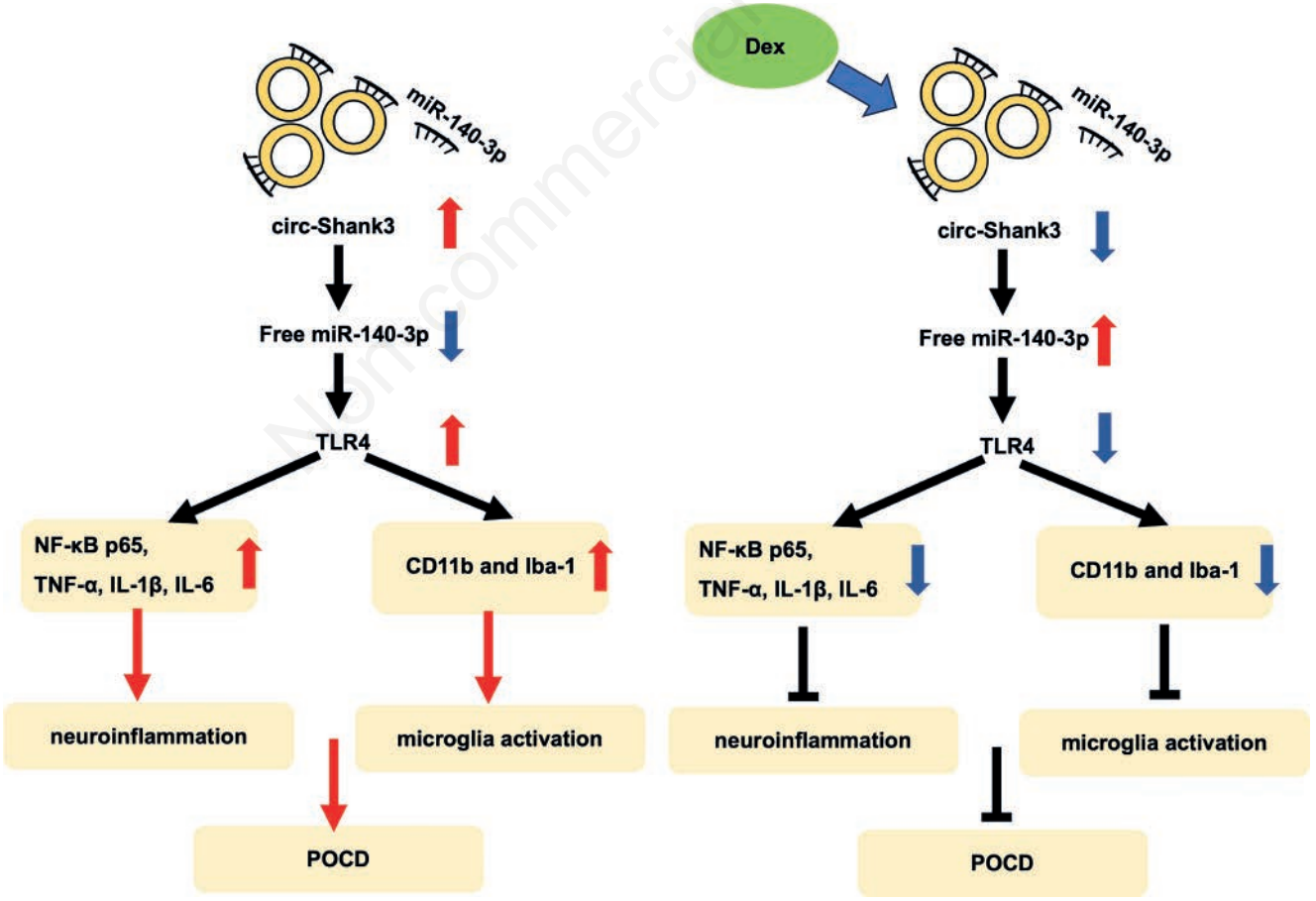

Figure 6. A schematic model of Dex functions in POCD. Dex could attenuate neuroinflammation and microglia activation in LPS-treated BV2 cells by modulating circ-Shank3/miR-140-3p/TLR4/NF-κB axis.

In this study, dual-luciferase reporter assays verified that circ-Shank3 could act as the sponge of miR-140-3p. Meanwhile, TLR4 is a potential binding target of miR-140-3p. Zhou *et al.* found that Dex could attenuate LPS-induced inflammatory response in BV2 cells through regulating TLR4/NF-κB pathway.[36] Additionally, Dex obviously ameliorated cognitive dysfunction in aged POCD mice *via* suppressing TLR4/NF-κB signaling.[37] Our results showed that Dex treatment significantly reduced TLR4 and p65 protein levels in LPS-treated BV2 cells. As expected, circ-Shank3 siRNA1 further reduced TLR4 and p65 levels in LPS-treated BV2 cells in the presence of Dex, whereas these phenomena were reversed by miR-140-3p inhibitor. To summarize, Dex could attenuate neuroinflammation in LPS-treated BV2 cells by modulating circ-Shank3/miR-140-3p/TLR4/NF-κB axis (Figure 6).

In conclusion, our results found that Dex could attenuate the neuroinflammation and microglia activation in LPS-treated BV2 cells *via* targeting circ-Shank3/miR-140-3p/TLR4 axis. For the first time, we investigated the relationship between Dex and circ-Shank3/miR-140-3p/TLR4 axis in POCD. Our results might shed new light on the mechanism of Dex for the treatment of POCD.

References

1. Lin X, Chen Y, Zhang P, Chen G, Zhou Y, Yu X. The potential mechanism of postoperative cognitive dysfunction in older people. Exp Gerontol 2020;130:110791.
2. Qiu LL, Pan W, Luo D, Zhang GF, Zhou ZQ, Sun XY, et al. Dysregulation of BDNF/TrkB signaling mediated by NMDAR/Ca(2+)/calpain might contribute to postoperative cognitive dysfunction in aging mice. J Neuroinflammation 2020;17:23.
3. Borchers F, Spies CD, Feinkohl I, Brockhaus WR, Kraft A, Kozma P, et al. Methodology of measuring postoperative cognitive dysfunction: a systematic review. Br J Anaesth 2021; 126:1119-27.
4. Yang XD, Wang LK, Wu HY, Jiao L. Effects of prebiotic galacto-oligosaccharide on postoperative cognitive dysfunction and neuroinflammation through targeting of the gut-brain axis. BMC Anesthesiol 2018;18:177.
5. Subramaniyan S, Terrando N. Neuroinflammation and perioperative neurocognitive disorders. Anesth Analg 2019;128:781-8.
6. Luo T, Hao YN, Lin DD, Huang X, Wu AS. Ginkgolide B improved postoperative cognitive dysfunction by inhibiting microgliosis-mediated neuroinflammation in the hippocampus of mice. BMC Anesthesiol 2022;22:229.
7. Sun L, Yong Y, Wei P, Wang Y, Li H, Zhou Y, et al. Electroacupuncture ameliorates postoperative cognitive dysfunction and associated neuroinflammation via NLRP3 signal inhibition in aged mice. CNS Neurosci Ther 2022;28:390-400.
8. Zhou H, Luo T, Wei C, Shen W, Li R, Wu A. RAGE antagonism by FPS-ZM1 attenuates postoperative cognitive dysfunction through inhibition of neuroinflammation in mice. Mol Med Rep 2017;16:4187-94.
9. Bao Y, Zhu Y, He G, Ni H, Liu C, Ma L, et al. Dexmedetomidine attenuates neuroinflammation in LPS-stimulated BV2 microglia cells through upregulation of miR-340. Drug Des Devel Ther. 2019;13:3465-75.
10. Wang YL, Zhang Y, Cai DS. Dexmedetomidine ameliorates postoperative cognitive dysfunction via the microRNA-381-mediated EGR1/p53 axis. Mol Neurobiol 2021;58:5052-66.
11. Zhou WY, Cai ZR, Liu J, Wang DS, Ju HQ, Xu RH. Circular RNA: metabolism, functions and interactions with proteins. Mol Cancer 2020;19:172.
12. Feng H, Yousuf S, Liu T, Zhang X, Huang W, Li A, et al. The comprehensive detection of miRNA and circRNA in the regulation of intramuscular and subcutaneous adipose tissue of Laiwu pig. Sci Rep 2022;12:16542.
13. Ni S, Jiang T, Hao S, Luo P, Wang P, Almatari Y, et al. circRNA expression pattern and ceRNA network in the pathogenesis of aseptic loosening after total hip arthroplasty. Int J Med Sci 2021;18:768-77.
14. Qian X, Zheng S, Yu Y. CircUBE3B high expression participates in sevoflurane-induced human hippocampal neuron injury via targeting miR-326 and regulating MYD88 expression. Neurotox Res 2023;41:16-28.
15. Cao C, Deng F, Hu Y. Dexmedetomidine alleviates postoperative cognitive dysfunction through circular RNA in aged rats. 3 Biotech 2020;10:176.
16. Zhang J, Yin J, Chen X, Mao X, Xu J, Cheng R, et al. Down-regulation of miR-140-3p can alleviate neonatal repetitive pain in rats via inhibiting TGF-β3. Biochem Biophys Res Commun 2019;515:627-35.
17. Cheng F, Qin W, Yang AX, Yan FF, Chen Y, Ma JX. Propofol alleviates neuropathic pain in chronic constriction injury rat models via the microRNA-140-3p/Jagged-1 peptide/Notch signaling pathway. Synapse 2021;75:e22219.
18. Wu Z, Tan J, Lin L, Zhang W, Yuan W. microRNA-140-3p protects hippocampal neuron against pyroptosis to attenuate sevoflurane inhalation-induced post-operative cognitive dysfunction in rats via activation of HTR2A/ERK/Nrf2 axis by targeting DNMT1. Cell Death Discov 2022;8:290.
19. Wang Z, Huang C, Zhao C, Zhang H, Zhen Z, Xu D. Knockdown of LINC01385 inhibits osteoarthritis progression by modulating the microRNA-140-3p/TLR4 axis. Exp Ther Med 2021;22:1244.
20. Xu Y, Yang B, Hu Y, Lu L, Lu X, Wang J, et al. Wogonin prevents TLR4-NF-κB-medicated neuro-inflammation and improves retinal ganglion cells survival in retina after optic nerve crush. Oncotarget 2016;7:72503-17.
21. Zeng K, Chen X, Xu M, Liu X, Hu X, Xu T, et al. CircHIPK3 promotes colorectal cancer growth and metastasis by sponging miR-7. Cell Death Dis 2018;9:417.
22. Yu L, Sun L, Chen S. Protective effect of senegenin on splenectomy-induced postoperative cognitive dysfunction in elderly rats. Exp Ther Med 2014;7:821-6.
23. El-Sahar AE, Shiha NA, El Sayed NS, Ahmed LA. Alogliptin Attenuates lipopolysaccharide-induced neuroinflammation in mice through modulation of TLR4/MYD88/NF-κB and miRNA-155/SOCS-1 signaling pathways. Int J Neuropsychopharmacol 2021;24:158-69.
24. Tan X, Tu Z, Han W, Song X, Cheng L, Chen H, et al. Anticonvulsant and neuroprotective effects of dexmedetomidine on pilocarpine-induced status epilepticus in rats using a metabolomics approach. Med Sci Monit 2019;25:2066-78.
25. Tasbihgou SR, Barends CRM, Absalom AR. The role of dexmedetomidine in neurosurgery. Best Pract Res Clin Anaesthesiol 2021;35:221-9.
26. Zhang Y, Gao Q, Wu Z, Xue H, Liu B, Zhao P. Dexmedetomidine promotes hippocampal neurogenesis and improves spatial learning and memory in neonatal rats. Drug Des Devel Ther 2019;13:4439-49.
27. Lv H, Li Y, Cheng Q, Chen J, Chen W. Neuroprotective effects against cerebral ischemic injury exerted by dexmedetomidine via the HDAC5/NPAS4/MDM2/PSD-95 axis. Mol Neurobiol 2021;58:1990-2004.
28. Liu YF, Hu R, Zhang LF, Fan Y, Xiao JF, Liao XZ. Effects of dexmedetomidine on cognitive dysfunction and neuroinflammation via the HDAC2/HIF-1α/PFKFB3 axis in a murine

model of postoperative cognitive dysfunction. J Biochem Mol Toxicol 2022;36:e23044.
29. Colonna M, Butovsky O. Microglia function in the central nervous system during health and neurodegeneration. Annu Rev Immunol 2017;35:441-68.
30. Wolf SA, Boddeke HW, Kettenmann H. Microglia in physiology and disease. Annu Rev Physiol 2017;79:619-43.
31. Ismail EN, Jantan I, Vidyadaran S, Jamal JA, Azmi N. Phyllanthus amarus prevents LPS-mediated BV2 microglial activation via MyD88 and NF-κB signaling pathways. BMC Complement Med Ther 2020;20:202.
32. Phillips TEJ, Maguire E. Phosphoinositides: roles in the development of microglial-mediated neuroinflammation and neurodegeneration. Front Cell Neurosci 2021;15:652593.
33. Cardozo PL, de Lima IBQ, Maciel EMA, Silva NC, Dobransky T, Ribeiro FM. Synaptic elimination in neurological disorders. Curr Neuropharmacol 2019;17:1071-95.
34. Ha Sen Ta N, Nuo M, Meng QT, Xia ZY. The pathway of Let-7a-1/2-3p and HMGB1 mediated dexmedetomidine inhibiting microglia activation in spinal cord ischemia-reperfusion injury mice. J Mol Neurosci 2019;69:106-14.
35. Zhang MX, Lin JR, Yang ST, Zou J, Xue Y, Feng CZ, et al. Characterization of circRNA-associated-ceRNA networks involved in the pathogenesis of postoperative cognitive dysfunction in aging mice. Front Aging Neurosci 2022;14:727805.
36. Zhou XY, Liu J, Xu ZP, Fu Q, Wang PQ, Zhang H. Dexmedetomidine inhibits the lipopolysaccharide-stimulated inflammatory response in microglia through the pathway involving TLR4 and NF-κB. Kaohsiung J Med Sci 2019;35:750-6.
37. Zhou XY, Liu J, Xu ZP, Fu Q, Wang PQ, Wang JH, et al. Dexmedetomidine ameliorates postoperative cognitive dysfunction by inhibiting Toll-like receptor 4 signaling in aged mice. Kaohsiung J Med Sci 2020;36:721-31.

Received: 4 May 2023. Accepted: 13 June 2023.

Licensee PAGEPress, Italy
European Journal of Histochemistry 2023; 67:3766
doi:10.4081/ejh.2023.3766